HINGE MOMENT COEFFICIENT DERIVATIVES FOR TRAILING-EDGE CONTROLS ON WINGS AT SUBSONIC SPEEDS

1. NOTATION AND UNITS (see Sketch 1.1)

		SI	British
A	aspect ratio		
$(a_1)_0$	lift-curve slope with angle of attack for two-dimensional section in incompressible flow	rad^{-1}	rad^{-1}
$(a_2)_0$	lift-curve slope with control deflection for two-dimensional section in incompressible flow	rad^{-1}	rad^{-1}
b_1	hinge moment coefficient derivative $\partial C_H/\partial\alpha$	rad^{-1}	rad^{-1}
$(b_1)_0$	value of b_1 for two-dimensional section in incompressible flow	rad^{-1}	rad^{-1}
Δb_1	contribution from induced camber to b_1	rad^{-1}	rad^{-1}
b_2	hinge moment coefficient derivative $\partial C_H/\partial\delta$	rad^{-1}	rad^{-1}
b_2'	hinge moment coefficient derivative $\partial C_H/\partial\delta'$	rad^{-1}	rad^{-1}
$(b_2)_0$	value of b_2 for two-dimensional section in incompressible flow	rad^{-1}	rad^{-1}
Δb_2	contribution from induced camber to b_2	rad^{-1}	rad^{-1}
C_H	hinge moment coefficient for control, $H/\tfrac{1}{2}\rho V^2 \bar{c}_f^2 s_f$		
C_L	lift coefficient for wing, $L/\tfrac{1}{2}\rho V^2 S$		
c	wing chord	m	ft
c'	wing chord measured normal to wing quarter-chord line	m	ft
c_b'	control balance chord forward of hinge line measured normal to wing quarter-chord line	m	ft
c_f	control chord aft of hinge line	m	ft
c_f'	control chord aft of hinge line measured normal to wing quarter-chord line	m	ft
$\bar{c}_f$	geometric mean control chord aft of hinge line, $\displaystyle\int_{\eta_i}^{\eta_o} c_f\,d\eta$	m	ft

$\overline{\overline{c}}_f$	aerodynamic mean control chord aft of hinge line, $$\int_{\eta_i}^{\eta_o} c_f^2 \, d\eta / \overline{c}_f$$	m	ft
F_B	factor on induced camber contributions to allow for control balance		
G_1, G_2, G_3	functions used in calculation of induced camber contribution, see Equations (3.5) and (3.6)	rad^{-1}	rad^{-1}
H	hinge moment	N m	lbf ft
K	correction factor for rectangular wing, see Section 3.4		
L	lift	N	lbf
M	Mach number		
R	Reynolds number based on wing mean chord		
S	wing area	m^2	ft^2
s	wing semispan	m	ft
s_f	control span, $s_f = s(\eta_o - \eta_i)$	m	ft
t	maximum thickness of wing section	m	ft
t_h	thickness of control at hinge line	m	ft
V	free-stream velocity	m/s	ft/s
α	angle of attack	rad	rad
α_i	mean induced angle of attack	rad	rad
β	compressibility parameter, $(1 - M^2)^{\frac{1}{2}}$		
δ	control deflection angle measured in plane parallel to plane of symmetry	rad	rad
δ'	control deflection angle measured in plane normal to hinge line	rad	rad
$\Lambda_{\frac{1}{4}}$	sweep angle of wing quarter-chord line	deg	deg
$\Lambda_{\frac{1}{2}}$	sweep angle of wing half-chord line	deg	deg
Λ_h	sweep angle of control hinge-line	deg	deg
η	spanwise distance from wing centre-line as fraction of semispan		

η_i, η_o	values of η at inboard and outboard limits of aileron at hinge line		
λ	ratio of wing tip chord to wing centre-line chord		
ρ	density of air	kg/m^3	slug/ft^3
τ'	section trailing-edge angle in plane normal to quarter-chord line	deg	deg

Superscript

$*$ as in $(a_1)_0^*$ denotes properties for a 'standard' section for which $\tau' = 2\tan^{-1}(t/c')$

Subscript

T as in $(a_1)_{0T}$ denotes theoretical value
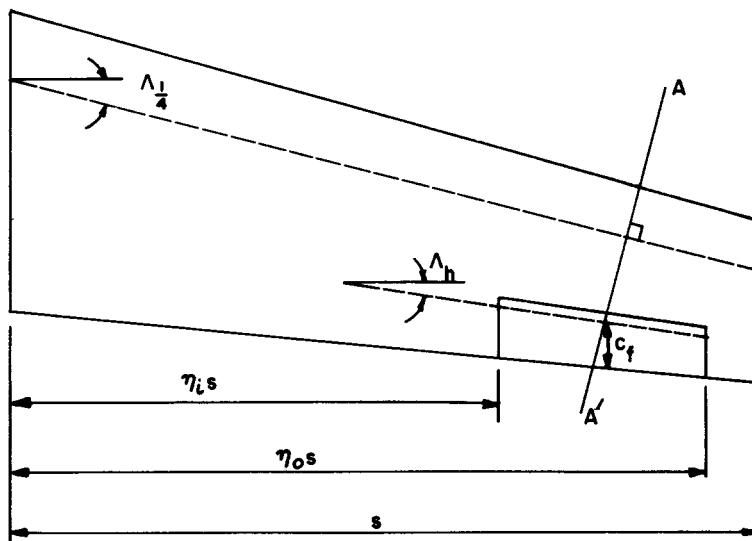
Planform geometry

AA$'$ normal to quarter-chord line and passing through mid-span of control
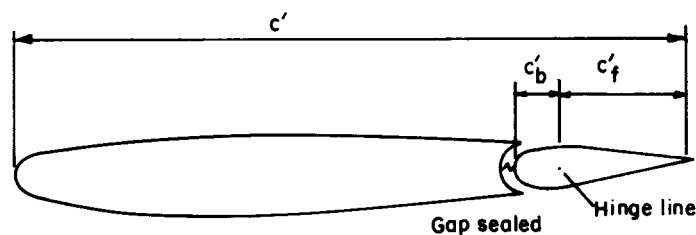
Section A A$'$

Sketch 1.1   Planform and section geometry

2. INTRODUCTION

This Item provides a method for estimating the hinge moment coefficient derivatives b_1 and b_2 for full-span and part-span sealed controls on swept and unswept wings at speeds where the flow over the wing is wholly subsonic and fully attached. It may also be used for controls on tailplanes or fins. The method follows the traditional approach for a wing of finite aspect ratio, whereby the two-dimensional sectional values are corrected for the effects of induced angle of attack and induced camber, see Derivations 1, 2, 11, 12 and 18 for example. The basic equations for the derivatives are essentially in the form of lifting-line theory, but with lifting-surface theories used to give a better evaluation of the induced angle of attack and to provide the important additional contribution due to induced camber. The equations permit ready substitution of known two-dimensional characteristics.

None of the various published versions of the above technique is sufficiently comprehensive in its theoretical calculations to cover in a satisfactory manner all configurations of interest. The method in this Item follows Derivation 18 in its treatment of wing sweep, which was based on a successful modification to the earlier work of Derivation 11. The presence of control balance is allowed for by adapting the theoretical calculations made in Derivation 2 for unswept wings. Empirical corrections are presented for part-span effects for controls that extend from a general inboard station η_i to near the wing tip, $\eta_o \geq 0.9$. The two-dimensional properties of the wing and control are assumed to be effectively constant over the span of the control. Prandtl-Glauert similarity parameters are employed to model the first order effects of compressibility at low to moderate subsonic speeds.

Item No. Aero C.04.01.00 (Derivation 29) provides a general introduction to the treatment of control hinge moment coefficient derivatives within the Aerodynamics Sub-series. It should be consulted for a brief description of the individual Items that are available and their inter-relationship. In addition, it gives qualitative guidance on the effects of control geometry and flow conditions on the range of linearity of hinge moment characteristics.

3. METHOD

3.1 Basic Equations

In incompressible flow the derivatives for a finite wing are related to the section values normal to the wing quarter-chord line by the equations

$$b_1 = (b_1)_0 \left(1 - \frac{\alpha_i}{\alpha} \right) \cos\Lambda_{1/4} \cos\Lambda_h + \Delta b_1 \tag{3.1}$$

and

$$b_2 = \left((b_2)_0 - \frac{\alpha_i}{\delta}(b_1)_0 \right) \cos\Lambda_{1/4} \cos\Lambda_h + \Delta b_2 , \tag{3.2}$$

where α_i is the mean induced angle of attack and Δb_1 and Δb_2 are induced camber contributions. These equations make the assumption that the angle α_i is constant across the span, which is a reasonable assumption for wings that are approximately elliptically loaded. For loadings that depart significantly from the elliptical a spanwise integration with α_i as a function of η is necessary, as described in Derivation 2 or Item No. Aero C.04.01.06 (Derivation 28). However, a relatively simple correction is possible for a rectangular wing that has constant two-dimensional properties, see Section 3.4.

3.2 Derivative b_1

The assumptions made in Derivation 18 lead to the substitution

$$\frac{\alpha_i}{\alpha} = 1 - \frac{\mathrm{d}C_L/\mathrm{d}\alpha}{(a_1)_0 \cos\Lambda_{1/4}}, \tag{3.3}$$

where $(a_1)_0$ is the two-dimensional lift-curve slope for the section normal to the wing quarter-chord line and $\mathrm{d}C_L/\mathrm{d}\alpha$ is the wing lift-curve slope estimated by lifting-surface theory. Values of $\mathrm{d}C_L/\mathrm{d}\alpha$ can be obtained from Item No. 70011 (Derivation 34). As in Derivation 20, for example, Prandtl-Glauert similarity parameters are incorporated to allow for first-order compressibility effects. With $\mathrm{d}C_L/\mathrm{d}\alpha$ calculated at the Mach number of interest, the general form for b_1 becomes

$$b_1 = \frac{(b_1)_0}{(a_1)_0}\left(\frac{\mathrm{d}C_L}{\mathrm{d}\alpha}\right)\cos\Lambda_h + \Delta b_1. \tag{3.4}$$

In this Item the correction Δb_1 is evaluated as

$$\Delta b_1 = G_1 + G_2, \tag{3.5}$$

where G_1 is the theoretically based contribution for a full-span control and G_2 is a purely empirical correction for part-span effects.

Lifting-surface values of G_1 for a plain control in incompressible flow were calculated in Derivation 18 for $2 \leq A \leq 6$ and $0 \leq \Lambda_{1/4} \leq 45°$. These are reproduced in Figure 1 where $2\pi\beta G_1/F_B(a_1)_0\cos\Lambda_h$ is given in three carpets as a function of $(1/\beta)\tan\Lambda_{1/4}$ and βA for values of the control chord ratio measured normal to the quarter-chord line, $c_f'/c' = 0.2, 0.3$ and 0.4. The data for unswept wings have been slightly adjusted to be compatible with the data for unswept wings given in Derivation 2 as these covered higher aspect ratios. For swept wings, extrapolations above $\beta A = 6$ have been made by taking the form of the variation for the unswept wing as a guide and noting that, for all sweep angles, G_1 must tend to zero as βA becomes very large. The factor F_B allows for control balance and has been deduced from the data given in Derivation 2 for nose-balanced and internally-balanced controls on unswept wings. For those two types of control F_B is given in Figure 2 as a function of c_f'/c' and balance c_b'/c_f'. For a plain control F_B is unity.

The empirical part-span correction G_2 is obtained from Figure 3 where $2\pi\beta G_2/F_B(a_1)_0\cos\Lambda_h$ is given in a carpet as a function of η_i and $A\tan\Lambda_{1/2}$. It is assumed that $\eta_o \geq 0.9$.

3.3 Derivative b_2

In the evaluation of b_2 given in Derivation 18 for full-span controls, some necessary simplifications were made to facilitate the lifting-surface calculations of the control-deflected loadings and only a partial evaluation of the induced effects was performed. Comparisons with experimental data showed that the overall contribution of the neglected components was acceptably small. However, although the resulting equation for b_2 resembles Equation (3.2) the approximation is such that the separate effects of induced angle of attack and induced camber cannot be identified. The equation for b_2 is

$$b_2 = \left((b_2)_0 - \frac{(a_2)_0}{(a_1)_0}(b_1)_0\right)\frac{\cos\Lambda_h}{(\beta^2 + \tan^2\Lambda_{1/4})^{1/2}} + \frac{(a_2)_0}{(a_1)_0}(b_1 + G_3), \tag{3.6}$$

where the function G_3 has been introduced in this Item to provide a further empirical allowance for part-span effects on the induced camber contribution, in addition to that made in b_1. Similarity parameters are again introduced to allow for the effects of compressibility. The lift-curve slope with control deflection $(a_2)_0$ is for a section normal to the wing quarter-chord line and a control chord ratio c_f'/c'. Figure 4 gives $2\pi\beta G_3/F_B(a_1)_0\cos\Lambda_h$ as a function of η_i. It is assumed that $\eta_o \geq 0.9$.

For control deflection angles measured normal to the hinge line, the hinge moment coefficient derivative is

$$\frac{\partial C_H}{\partial \delta'} = b_2' = b_2\cos\Lambda_h. \tag{3.7}$$

3.4 Rectangular Wing

For a rectangular wing with uniform section and control geometry, Item No. Aero C.04.01.06 contains information on the spanwise variation of the ratio of α_i for a rectangular wing to the value of α_i for an elliptically-loaded wing. This information has been used to deduce a simple factor K to modify Equations (3.4) and (3.6). The factor is simply the mean value of the α_i ratio over the span of the control. Figure 5 shows K as a function η_i for $\eta_o \geq 0.9$. The equations for b_1 and b_2 become

$$b_1 = (b_1)_0\left\{1 - K\left(1 - \frac{dC_L/d\alpha}{(a_1)_0}\right)\right\} + \Delta b_1 \tag{3.8}$$

and
$$b_2 = \frac{1}{\beta}\left((b_2)_0 - K\frac{(a_2)_0}{(a_1)_0}(b_1)_0\right) + \frac{(a_2)_0}{(a_1)_0}(b_1 + G_3). \tag{3.9}$$

With K taken from Figure 5, the equations are otherwise evaluated as in Sections 3.2 and 3.3. If $K = 1$, Equations (3.8) and (3.9) reduce to Equations (3.4) and (3.6) with $\Lambda_{\frac{1}{4}} = \Lambda_h = 0$. For a full-span control $K \approx 1$, but the correction becomes important for part-span controls.

3.5 Sectional Properties

The sectional properties that are required in the calculation of b_1 and b_2 can be obtained as indicated in the table, or experimental values may be substituted if they are known.

Parameter	Item No. Aero	Derivation
$(a_1)_0$	W.01.01.05	30
$(a_2)_0$	C.01.01.03	31
$(b_1)_0$	C.04.01.01 (plain control)	32
$(b_2)_0$	C.04.01.02 (plain control)	33
Corrections to $(b_1)_0$	$\big\{$ C.04.01.03 (nose balance)	26
and $(b_2)_0$ for balance	C.04.01.04 (Irving internal balance)	27

The use of these Derivations is illustrated in the Example (see Section 6).

4. ACCURACY AND APPLICABILITY

4.1 Accuracy

Sketches 4.1 and 4.2 demonstrate the overall accuracy of prediction at low speeds using test data from Derivations 2 and 4 to 25. In general, b_1 is predicted to within about ± 0.05 rad^{-1} and b_2 to within ± 0.07 rad^{-1}. As would be expected, estimated values are usually more reliable when known two-dimensional section properties are available. The method gives best estimates for full-span controls on unswept wings, but there is otherwise no general trend within the overall scatter. For comparison, the accuracy quoted in Item Nos Aero C.04.01.01 and 02 for $(b_1)_0$ and $(b_2)_0$ is ± 0.05 rad^{-1}.

The use of similarity parameters provides a reasonable representation of compressibility effects for Mach numbers at which the flow over the wing is wholly subsonic and fully attached, provided the section profiles are thin, $t/c' \leq 0.14$ say, and the controls have straight-tapered profiles aft of the hinge line. The variations with Mach number are small in these cases. The method is unsatisfactory for predicting the larger variations associated with thicker sections and more complex control profiles. Examples of the different variations with Mach number that are displayed by various controls are contained in Derivation 9.

The empirical part-span correction for b_1 differs considerably from the theoretical one given for unswept wings in Derivations 3 and 12. Indeed, as demonstrated by the form of G_2, best predictions are achieved with no correction for unswept wings, although one is needed for swept wings. The further empirical part-span correction introduced in the calculation of b_2, namely G_3, could only be defined crudely within a considerable scatter of experimental results but it does remove a bias that would otherwise exist in the prediction. For both part-span corrections, particular notice was taken of the results of parametric tests in which the control span was altered systematically.

4.2 Applicability

The derivatives b_1 and b_2 are defined over small ranges of angle of attack and control deflection, where the hinge moment coefficient varies linearly. A general discussion on factors affecting the extent of the linear range is given in the introductory Item No. Aero C.04.01.00 (Derivation 29).

An indication of the range of wing and control geometries covered in the development of the method is given in the table. The method applies to sealed controls with streamwise side-edges. If the side edges are normal to a swept hinge-line then there can be a significant change in b_2, although the effect on b_1 is small (Derivation 10).

Parameter	*Range*	*Parameter*	*Range*
A	2 to 8	t/c'	0.06 to 0.14
$\Lambda_{1/2}$	0 to 50°	τ'	6° to 20°
c_f'/c'	0.2 to 0.4	η_i	0 to 0.8

The main method in Sections 3.2 and 3.3 assumes that the wing loading is elliptical and that the wing and control two-dimensional properties are essentially constant over the span of the control. The modest departures from these conditions that are normally expected will not lead to undue errors in prediction. A simple modification is given in Section 3.4 for rectangular wings with constant two-dimensional properties. For the special case of full-span controls on unswept wings with a large spanwise variation in sectional properties the method of Item No. Aero C.04.01.06 (Derivation 28) may be used.

The method is based on an analysis of data on controls that extend to near the wing tip; therefore, it must be used with caution if applied to controls that are well inboard with η_o substantially less than 0.9.
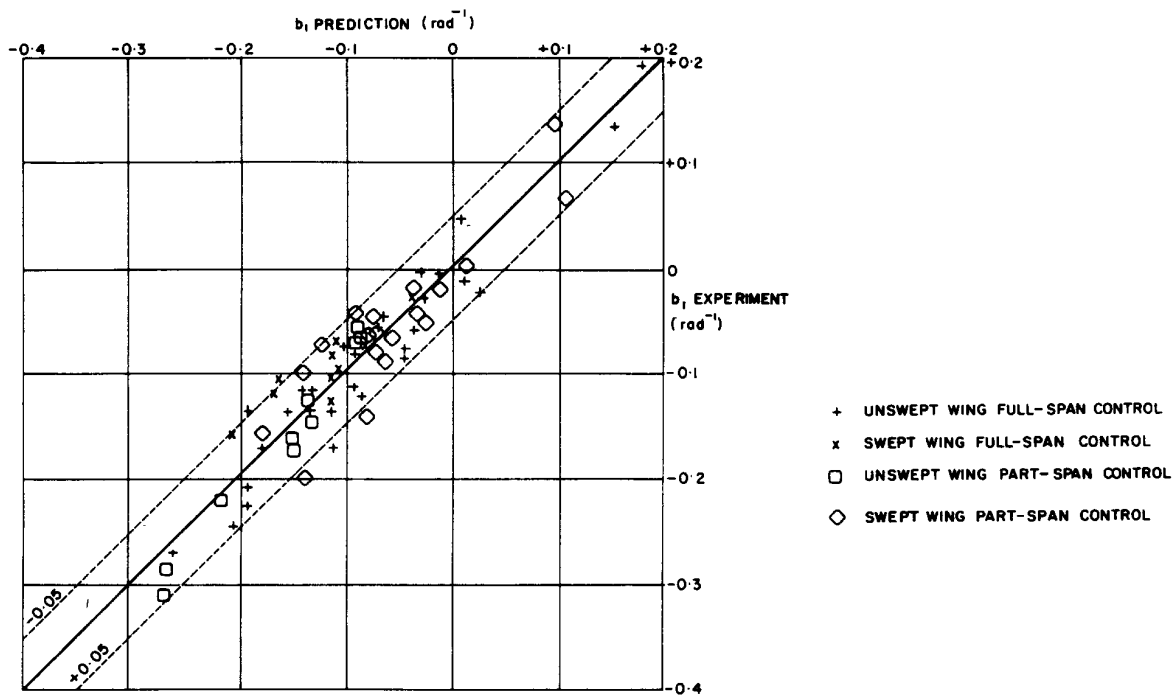
Sketch 4.1   Comparison of predicted and experimental values of b_1
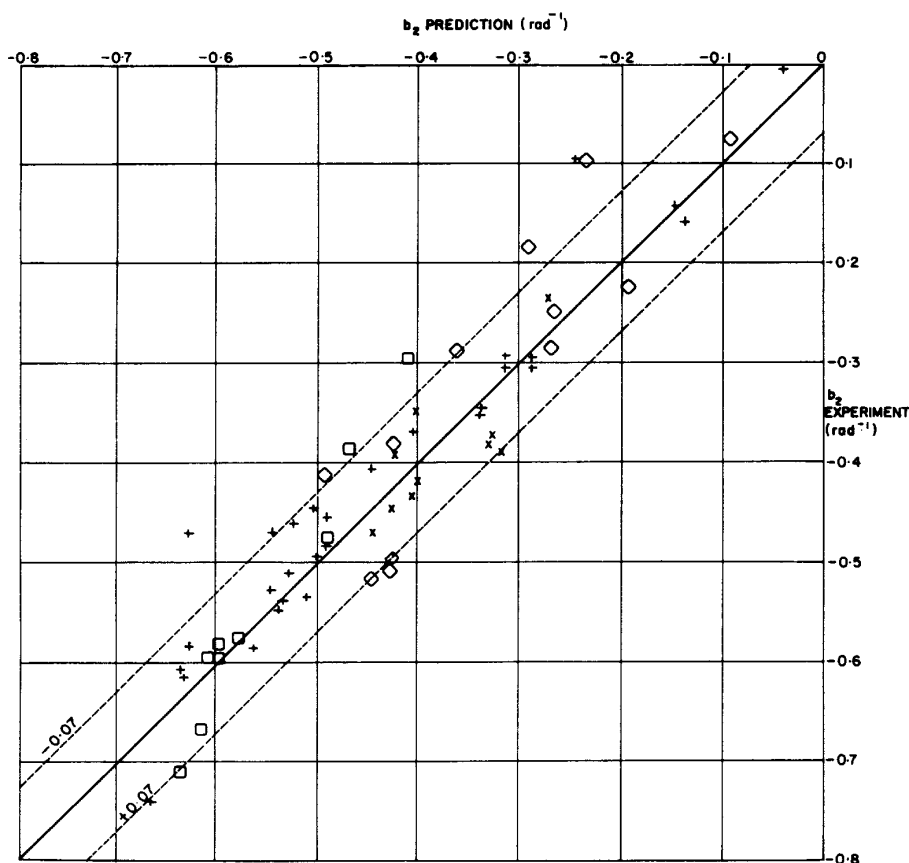
Sketch 4.2   Comparison of predicted and experimental values of b_2

5. **DERIVATION**

The Derivation lists selected sources that have assisted in the preparation of this Item.

1. SWANSON, R.S.
    PRIDDY, L. La V.
    Lifting-surface-theory values of the damping in roll and of the parameters used in estimating aileron stick forces. NACA ARR L5F23 (TIL 1017), 1945.

2. SWANSON, R.S.
    CRANDALL, S.H.
    Lifting-surface-theory aspect-ratio corrections to the lift and hinge-moment parameters for full-span elevators on horizontal tail surfaces. NACA tech. Note 1175, 1946. (Also as NACA Rep. 911, 1948.)

3. TOLL, T.A.
    Summary of lateral-control research. NACA tech. Note 1245, 1946.

4. BIELAT, R.P.
    Investigation at high speeds of a horizontal-tail model in the Langley 8-foot high-speed tunnel. NACA RM L6L10b (TIL 1156), 1947.

5. SCHUELLER, G.H.
    COOPER, M.
    Aerodynamic force characteristics at high speeds of a full-scale horizontal tail surface tested in the Langley 16-foot high-speed tunnel. NACA RM L7D08 (TIL 1184), 1947.

6. SCHULDENFREI, M.
    COMISAROW, P.
    GOODSON, K.W.
    Stability and control characteristics of an airplane model having a 45.1° swept-back wing with aspect ratio 2.50 and taper ratio 0.42 and a 42.8° swept-back horizontal tail with aspect ratio 3.87 and taper ratio 0.49. NACA RM L7B25 (TIL 1389), 1947.

7. FISCHEL, J.
    SCHNEITER, L.E.
    High-speed wind-tunnel investigation of high lift and aileron-control characteristics of an NACA 65-210 semispan wing. NACA tech. Note 1473, 1947.

8. MORRILL, C.P.
    BODDY, L.E.
    High-speed stability and control characteristics of a fighter airplane model with a swept-back wing and tail. NACA RM A7K28 (TIL 1915), 1948.

9. AXELSON, J.A.
    A summary of wind-tunnel data on the lift and hinge-moment characteristics of control surfaces up to a Mach number of 0.90. NACA RM A7L02 (TIL 1799), 1948.

10. FISCHEL, J.
    SCHNEITER, L.E.
    An investigation at low speed of a 51.3° sweptback semispan wing equipped with 16.7 per cent chord plain flaps and ailerons having various spans and three trailing-edge angles. NACA RM L8H20 (TIL 1988), 1948.

11. JONES, A.L.
    SLUDER, L.
    An application of Falkner's surface-loading method to predictions of hinge-moment parameters for swept-back wings. NACA tech. Note 1506, 1948.

12. TOLL, T.A.
    SCHNEITER, L.E.
    Approximate relations for hinge-moment parameters of control surfaces on swept wings at low Mach numbers. NACA tech. Note 1711, 1948.

13. SCHNEITER, L.E.
    NAESETH, R.L.
    Wind-tunnel investigation at low speed of the lateral control characteristics of ailerons having three spans and three trailing-edge angles on a semispan wing model. NACA tech. Note 1738, 1948.

14. GRAHAM, R.R.
    KOVEN, W.

    Lateral-control investigation on a 37° sweptback wing of aspect ratio 6 at a Reynolds number of 6,800,000. NACA RM L8K12 (TIL 2073), 1949.

15. SCHNEITER, L.E.
    HAGERMAN, J.R

    Wind-tunnel investigation at high subsonic speeds of the lateral-control characteristics of an aileron and a stepped spoiler on a wing with leading edge swept back 51.3° . NACA RM L9D06 (TIL 2117), 1949.

16. BOLLECH, T.V.
    PRATT, G.L.

    Investigation of low-speed aileron control characteristics at a Reynolds number of 6,800,000 of a wing with leading edge swept back 42° with and without high-lift devices. NACA RM L9E24 (TIL 2164), 1949.

17. JOHNSON, H.S.
    HAGERMAN, J.R.

    Wind-tunnel investigation at low speed of the lateral control characteristics of an unswept untapered semispan wing of aspect ratio 3.13 equipped with various 25 per cent chord plain ailerons. NACA tech. Note 2199, 1950.

18. DODS, J.B.

    Estimation of low-speed lift and hinge-moment parameters for full-span trailing-edge flaps on lifting surfaces with and without sweepback. NACA tech. Note 2288, 1950.

19. HADAWAY, W.M.
    SALMI, R.J.

    Investigation of low-speed lateral control and hinge-moment characteristics of a 20 per chord plain aileron on a 47.7° swept back wing of aspect ratio 5.1 at a Reynolds number of 6.0×10^6 . NACA RM L51F22 (TIL 2918), 1951.

20. KOLBE, C.D.
    BANDETTINI, A.

    Investigation in the Ames 12-foot pressure wind tunnel of a model horizontal tail of aspect ratio 3 and taper ratio 0.5 having the quarter-chord line swept back 45° . NACA RM A51D02 (TIL 2780), 1951.

21. PFYL, F.A.

    Aerodynamic study of a wing-fuselage combination employing a wing swept back 63° – effectiveness of an inboard elevon as a longitudinal- and lateral-control device at subsonic and supersonic speeds. NACA RM A51I18 (TIL 2948), 1951.

22. DODS, J.B.
    TINLING, B.E.

    Summary of results of a wind-tunnel investigation of nine related horizontal tails. NACA tech. Note 3497, 1951.

23. RUNCKEL, J.F.
    HEISER, G.

    Normal-force and hinge-moment characteristics at transonic speeds of flap-type ailerons at three spanwise locations on a 4 per cent thick sweptback-wing-body model and pressure-distribution measurements on an inboard aileron. NASA tech. Note D-842, 1961.

24. JACOBS, P.F.

    Effect of aileron deflections on the aerodynamic characteristics of a subsonic energy-efficient transport. NASA tech. Paper 2478, 1985.

25. BAe

    Unpublished wind-tunnel data.

ESDU Items

26. ESDU

    Effect of nose balance on two-dimensional control hinge-moment coefficients. Item No. Aero C.04.01.03, ESDU International, 1949.

27. ESDU

    Effect of Irving internal balance on hinge-moment coefficient in two-dimensional flow. Item No. Aero C.04.01.04, ESDU International, 1949.

28. ESDU   Full-span control hinge moment coefficient derivatives in incompressible flow for unswept wings with allowance for spanwise variation of sectional properties. Item No. Aero C.04.01.06, ESDU International, 1949.

29. ESDU   Introduction to Data Items on control hinge moments. Item No. C.04.01.00, ESDU International, 1950.

30. ESDU   Slope of lift curve for two-dimensional flow. Item No. Aero W.01.01.05, ESDU International, 1955.

31. ESDU   Rate of change of lift coefficient with control deflection in incompressible two-dimensional flow, $(a_2)_0$. Item No. Aero C.01.01.03, ESDU International, 1956.

32. ESDU   Rate of change of hinge moment coefficient with incidence for a plain control in incompressible two-dimensional flow, $(b_1)_0$. Item No. Aero C.04.01.01, ESDU International, 1956.

33. ESDU   Rate of change of hinge moment coefficient with control deflection for a plain control in incompressible two-dimensional flow, $(b_2)_0$. Item No. Aero C.04.01.02, ESDU International, 1956.

34. ESDU   Lift-curve slope and aerodynamic centre position of wings in inviscid subsonic flow. Item No. 70011, ESDU International, 1970.

6.   EXAMPLE

Calculate the hinge moment derivatives for the control shown in Sketch 6.1. Assume a Mach number of 0.4 and a Reynolds number of 3.5×10^7 based on wing mean chord. The required geometric parameters are summarised in the table. The control has a nose balance with a rounded forward profile.
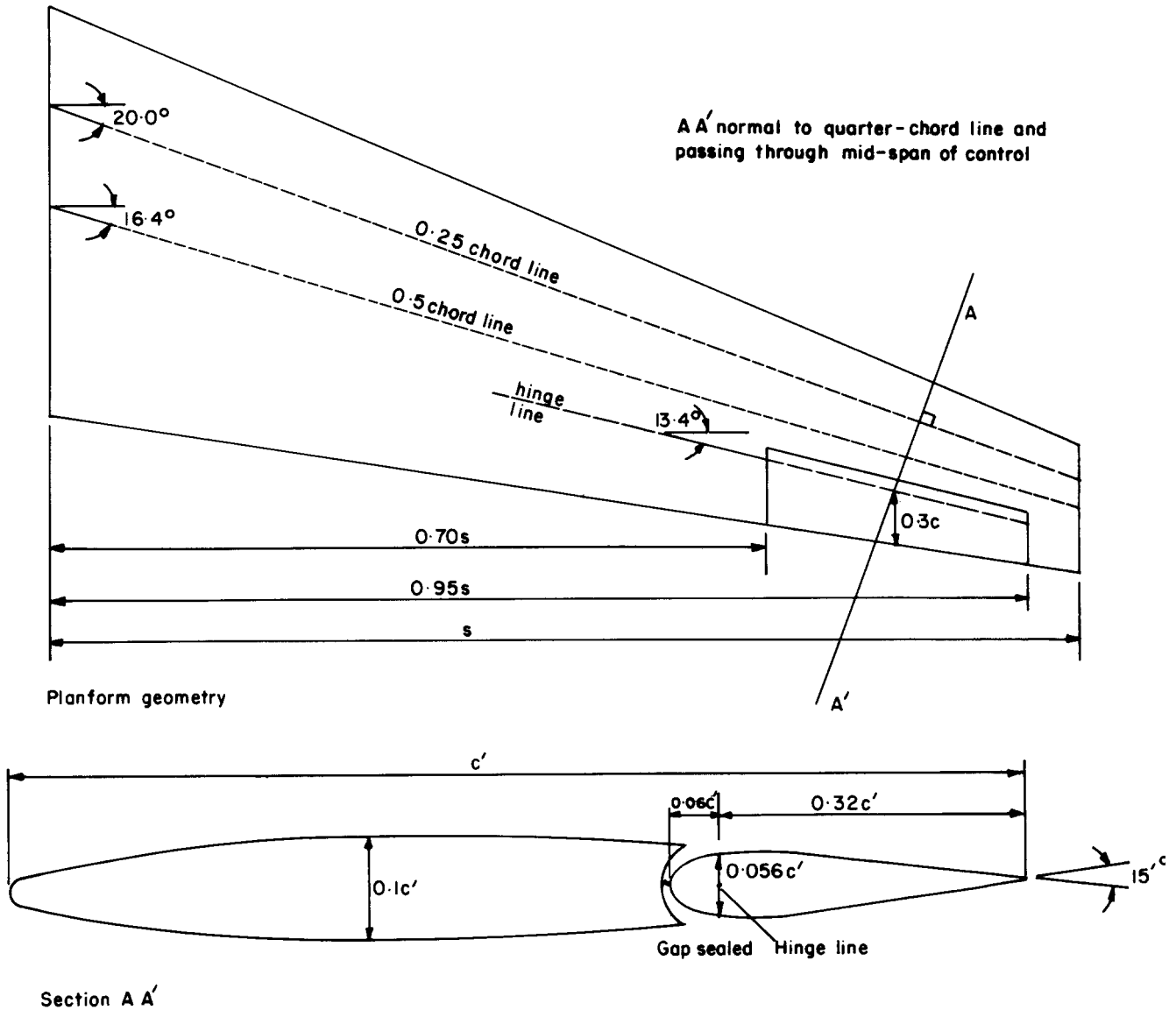
Sketch 6.1

	From planform geometry			*From section geometry*		
A	= 7.7	λ	= 0.3	τ'	= 15.0°	
$\Lambda_{1/4}$	= 20.0°	η_i	= 0.70	t/c'	= 0.1	
$\Lambda_{1/2}$	= 16.4°	η_o	= 0.95	c_b'/c'	= 0.06	
Λ_h	= 13.4°	c_f/c	= 0.30	c_f'/c'	= 0.32	

(i)   *Determine section properties* $(a_1)_0$, $(a_2)_0$, $(b_1)_0$, $(b_2)_0$.

If experimental data are available for section properties, go to Step *(ii)*.

From Item No. Aero W.01.01.05, with a Reynolds number $R = 3.5 \times 10^7$, a trailing-edge angle $\tau' = 15°$, a thickness chord ratio $t/c' = 0.10$, and an assumed boundary-layer transition point of $0.3 \; c'$,

$$\frac{(a_1)_0}{(a_1)_{0T}} = 0.883$$

and $(a_1)_{0T} = 6.788 \text{ rad}^{-1}$,

so $(a_1)_0 = 5.994 \text{ rad}^{-1}$.

From Item No. Aero C.01.01.03, with $c_f'/c' = 0.32$, $t/c' = 0.10$ and $(a_1)_0/(a_1)_{0T} = 0.883$,

$$(a_2)_{0T} = 4.600 \text{ rad}^{-1} ,$$

and $\dfrac{(a_2)_0}{(a_2)_{0T}} = 0.835$,

so $(a_2)_0 = 3.841 \text{ rad}^{-1}$.

The calculation of $(b_1)_0$ and $(b_2)_0$ requires corresponding values, denoted $(a_1)_0$* *etc*, for a 'standard' aerofoil section with $\tau' = 2\tan^{-1}(t/c')$. By again using Item Nos Aero W.01.01.05 and Aero C.01.01.03, with $\tau' = 2\tan^{-1}(0.10) = 11.4°$,

$$\frac{(a_1)_0{}^*}{(a_1)_{0T}{}^*} = 0.906$$

and $(a_1)_{0T}$* $= 6.781 \text{ rad}^{-1}$,

so $(a_1)_0$* $= 6.143 \text{ rad}^{-1}$.

Also $(a_2)_{0T}$* $= 4.600 \text{ rad}^{-1}$

and $\dfrac{(a_2)_0{}^*}{(a_2)_{0T}{}^*} = 0.862$,

so $(a_2)_0$* $= 3.965 \text{ rad}^{-1}$.

Then from Item No. Aero C.04.01.01 with $t/c' = 0.10$, $c_f'/c' = 0.32$ and $(a_1)_0$*$/(a_1)_{0T}$* $= 0.906$, for a plain unbalanced control in incompressible flow

$$- (b_1)_{0T}{}^* = 0.580 \text{ rad}^{-1}$$

and $\quad\quad \dfrac{(b_1)_0{}^*}{(b_1)_{0T}{}^*} = 0.795,$

so $\quad\quad \begin{aligned}(b_1)_0 &= (b_1)_0{}^* + 2[(a_1)_{0T}{}^* - (a_1)_0{}^*](\tan\tfrac{1}{2}\tau' - t/c') \\ &= -0.580 \times 0.795 + 2[6.781 - 6.143](\tan 7.5° - 0.10) \\ &= -0.421 \text{ rad}^{-1}.\end{aligned}$

Similarly, from Item No. Aero C.04.01.02 with $t/c' = 0.10$, $c_f'/c' = 0.32$ and $(a_2)_0{}^*/(a_2)_{0T}{}^* = 0.862$,

$\quad\quad -(b_2)_{0T}{}^* = 0.902 \text{ rad}^{-1}$

and $\quad\quad \dfrac{(b_2)_0{}^*}{(b_2)_{0T}{}^*} = 0.880,$

so $\quad\quad \begin{aligned}(b_2)_0 &= (b_2)_0{}^* + 2[(a_2)_{0T}{}^* - (a_2)_0{}^*](\tan\tfrac{1}{2}\tau' - t/c') \\ &= -0.902 \times 0.880 + 2[4.600 - 3.965](\tan 7.5° - 0.10) \\ &= -0.754 \text{ rad}^{-1}.\end{aligned}$

The control has a nose balance so Item No. Aero C.04.01.03 must be used to correct the values of b_1 and b_2 that have been calculated above for plain controls. (For an Irving internal balance see Item No. Aero C.04.01.04.)

With $t/c' = 0.10$, a round nose profile, and a balance ratio given by

$$[(c_b'/c_f')^2 - (\tfrac{1}{2}\, t_h/c_f')^2]^{1/2} = [(0.06/0.32)^2 - (\tfrac{1}{2} \times 0.056/0.32)^2]^{1/2} = 0.166,$$

Item No. Aero C.04.01.03 gives the ratio of balanced to plain control derivatives

$\quad\quad \dfrac{(b_1)_{0Bal}}{(b_1)_{0Plain}} = 0.89$

and $\quad\quad \dfrac{(b_2)_{0Bal}}{(b_2)_{0Plain}} = 0.78.$

Therefore, for the balanced control,

$\quad\quad (b_1)_0 = -0.421 \times 0.89 = -0.375 \text{ rad}^{-1}$

and $\quad\quad (b_2)_0 = -0.754 \times 0.78 = -0.588 \text{ rad}^{-1}.$

(ii)   *Calculate $\mathrm{d}C_L/\mathrm{d}\alpha$ for the wing*

For $M = 0.4$, $\beta = (1 - M^2)^{1/2} = 0.917$.

From Item No. 70011, with $\lambda = 0.3$, $A \tan \Lambda_{\frac{1}{2}} = 7.7 \tan 16.4° = 2.27$, and $\beta A = 0.917 \times 7.7 = 7.06$,

$$\frac{1}{A} \frac{dC_L}{d\alpha} = 0.630 \text{ rad}^{-1}$$

so

$$\frac{dC_L}{d\alpha} = 7.7 \times 0.630 = 4.851 \text{ rad}^{-1}.$$

(iii)   Calculate b_1

From Figure 1 with $\beta A = 7.06$, $c_f'/c' = 0.32$ and $(1/\beta)\tan\Lambda_{\frac{1}{4}} = (1/0.917)\tan 20° = 0.397$, the full-span induced camber contribution parameter is

$$\frac{2\pi\beta G_1}{F_B (a_1)_0 \cos\Lambda_h} = -0.008 \text{ rad}^{-1}.$$

For a nose-balanced control with $c_b'/c_f' = 0.06/0.32 = 0.188$ and $c_f'/c' = 0.32$, the balance factor F_B from Figure 2a is 0.935,

so

$$G_1 = -0.008 \times \frac{0.935 \times 5.994 \times \cos 13.4°}{2 \times \pi \times 0.917} = -0.008 \times 0.946 = -0.008 \text{ rad}^{-1}.$$

(Note that the bracketed numerical expression involved in evaluating G_1, G_2 and G_3 is dimensionless because $(a_1)_0$ is normalised by the presence of the theoretical thin aerofoil value 2π rad^{-1}.)

From Figure 3 with $A \tan \Lambda_{\frac{1}{2}} = 2.27$ and $\eta_i = 0.70$ the part-span induced camber contribution parameter is

$$\frac{2\pi\beta G_2}{F_B (a_1)_0 \cos\Lambda_h} = 0.070 \text{ rad}^{-1},$$

so

$$G_2 = 0.070 \times \frac{0.935 \times 5.994 \times \cos 13.4°}{2 \times \pi \times 0.917} = 0.070 \times 0.946 = 0.066 \text{ rad}^{-1}.$$

Therefore, from Equation (3.5)

$$\Delta b_1 = G_1 + G_2$$

$$= -0.008 + 0.066 = 0.058 \text{ rad}^{-1},$$

and from Equation (3.4)

$$b_1 = \frac{(b_1)_0}{(a_1)_0} \left(\frac{dC_L}{d\alpha} \right) \cos\Lambda_h + \Delta b_1$$

$$= \frac{-0.375}{5.994} \times 4.851 \times \cos 13.4° + 0.058 = -0.295 + 0.058 = -0.237 \text{ rad}^{-1}.$$

(iv)   *Calculate* b_2

From Figure 4 with $\eta_i = 0.7$ the parameter giving the further part-span induced camber contribution is

$$\frac{2\pi\beta G_3}{F_B(a_1)_0\cos\Lambda_h} = 0.105 \text{ rad}^{-1},$$

so $$G_3 = 0.105 \times \frac{0.935 \times 5.994 \times \cos 13.4°}{2 \times \pi \times 0.917} = 0.105 \times 0.946 = 0.099 \text{ rad}^{-1}.$$

Therefore, from Equation (3.6)

$$b_2 = \left((b_2)_0 - \frac{(a_2)_0}{(a_1)_0}(b_1)_0\right)\frac{\cos\Lambda_h}{(\beta^2 + \tan^2\Lambda_{1/4})^{1/2}} + \frac{(a_2)_0}{(a_1)_0}(b_1 + G_3)$$

$$= \left(-0.588 - \frac{3.841}{5.994}(-0.375)\right)\frac{\cos 13.4°}{(0.917^2 + \tan^2 20°)^{1/2}} + \frac{3.841}{5.994}(-0.237 + 0.099)$$

$$= -0.343 - 0.088 = -0.431 \text{ rad}^{-1}.$$

For control angles measured normal to the hinge line,

$$b_2' = b_2\cos\Lambda_h$$
$$= -0.431\cos 13.4°$$
$$= -0.419 \text{ rad}^{-1}.$$

The graphs show plots of $\dfrac{2\pi\,\beta\,G_1}{F_B\,(a_1)_0\,\cos\Lambda_h}$ (rad^{-1}) versus $(1/\beta)\tan\Lambda_{1/4}$ for various βA.

(a) $\dfrac{c'_f}{c'} = 0.2$

(b) $\dfrac{c'_f}{c'} = 0.3$

(c) $\dfrac{c'_f}{c'} = 0.4$
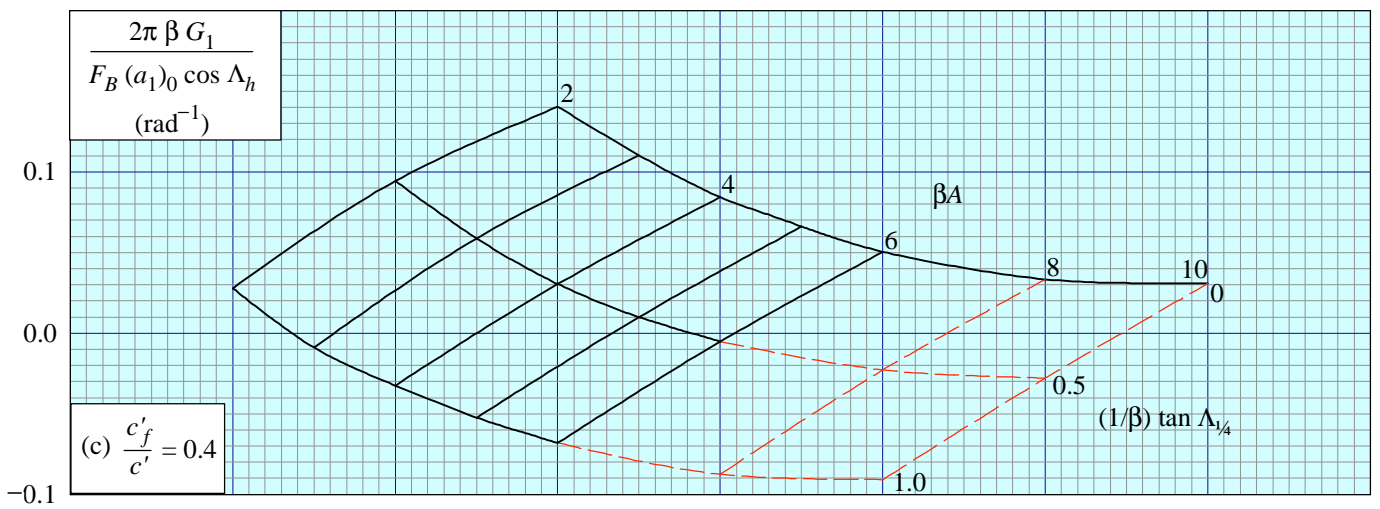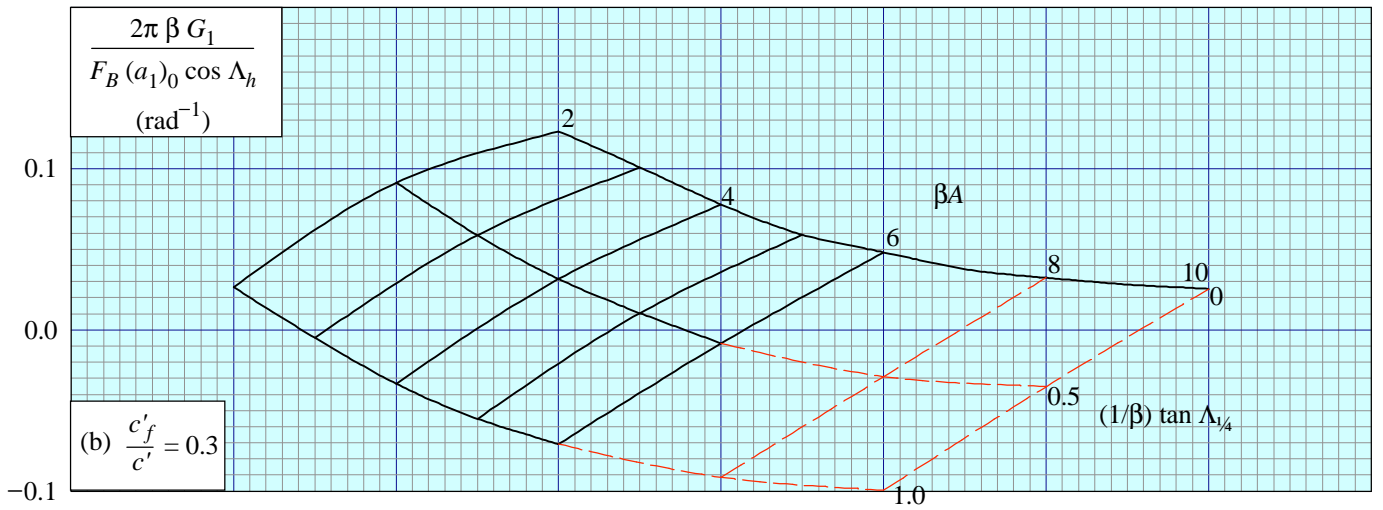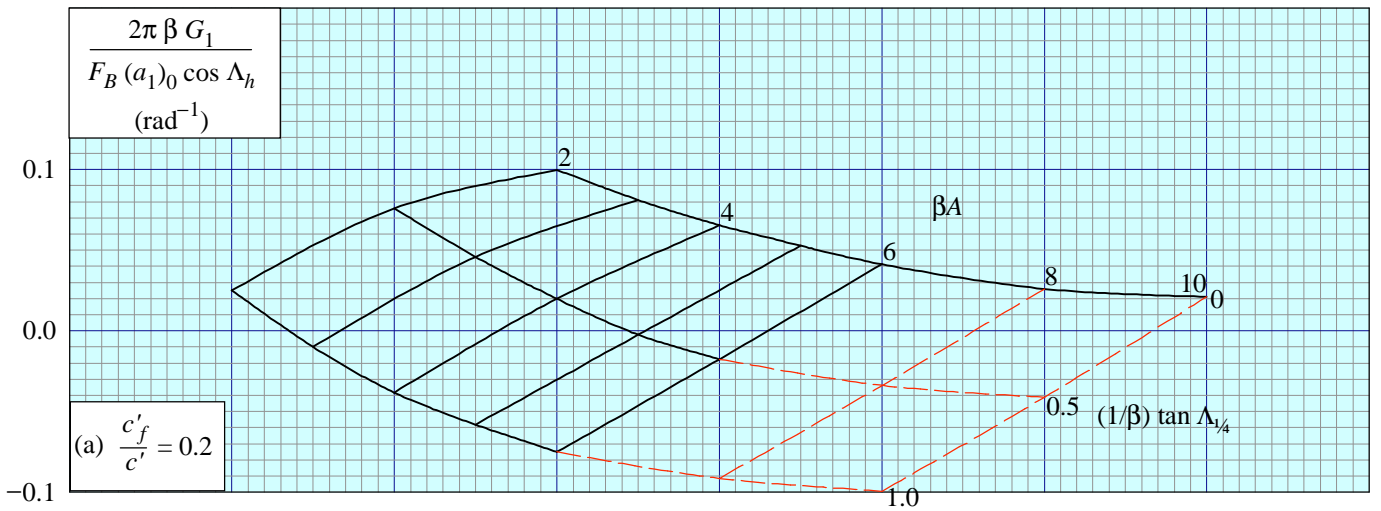
FIGURE 1 INDUCED CAMBER CONTRIBUTION FOR FULL-SPAN CONTROLS
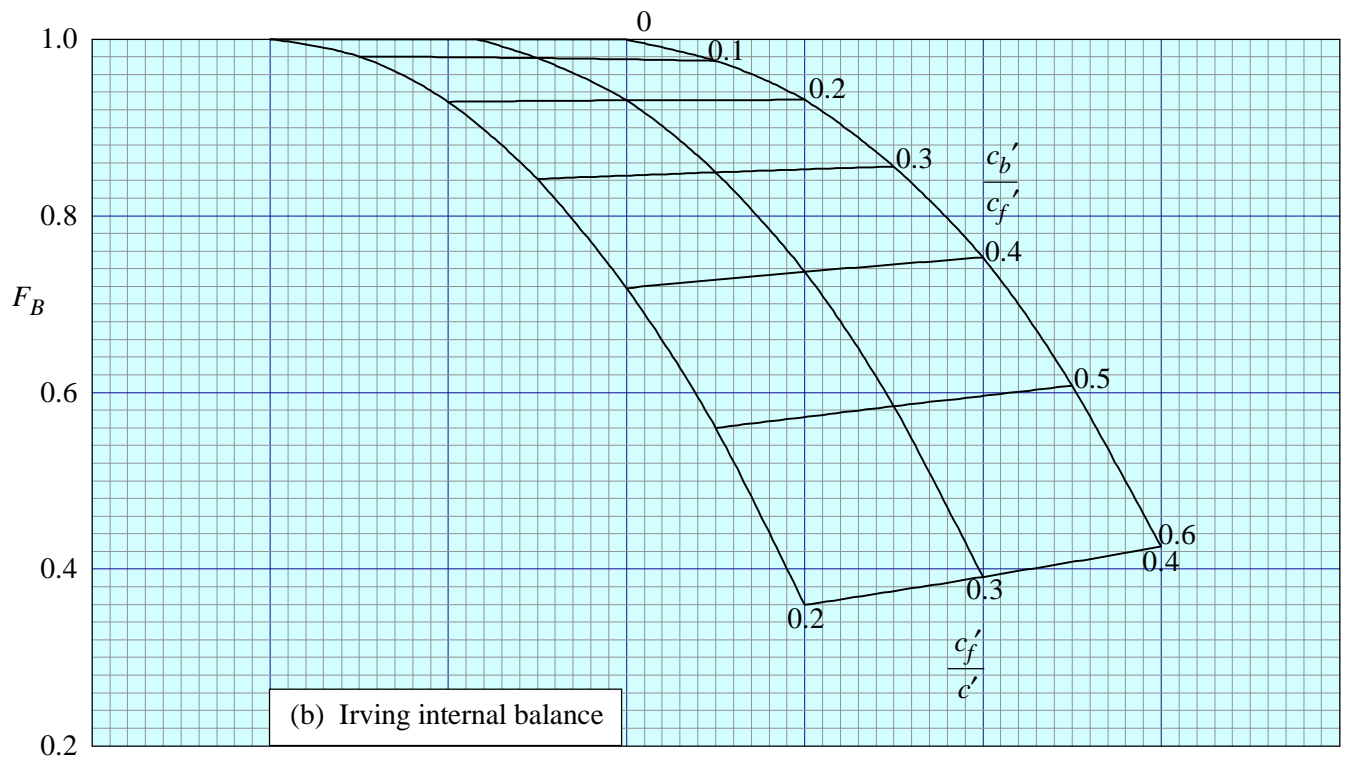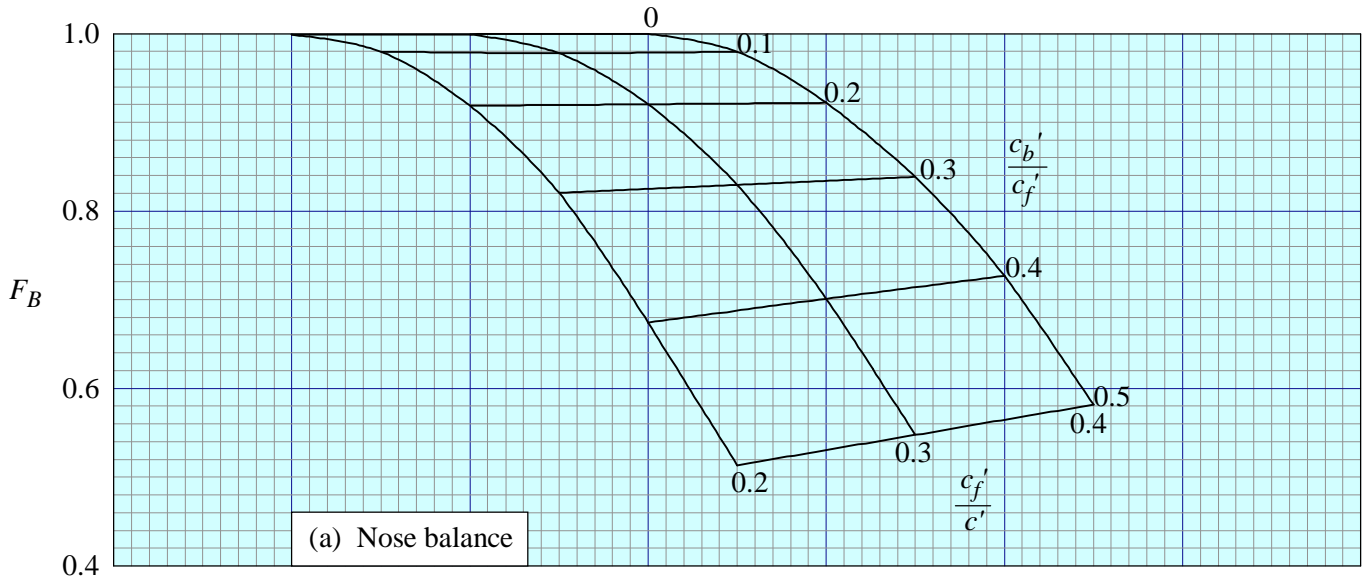
FIGURE 2 FACTOR ON INDUCED CAMBER CONTRIBUTION TO ALLOW FOR CONTROL BALANCE

$$\frac{2\pi\,\beta\,G_2}{F_B\,(a_1)_0\,\cos\Lambda_h}\ (\mathrm{rad}^{-1})$$
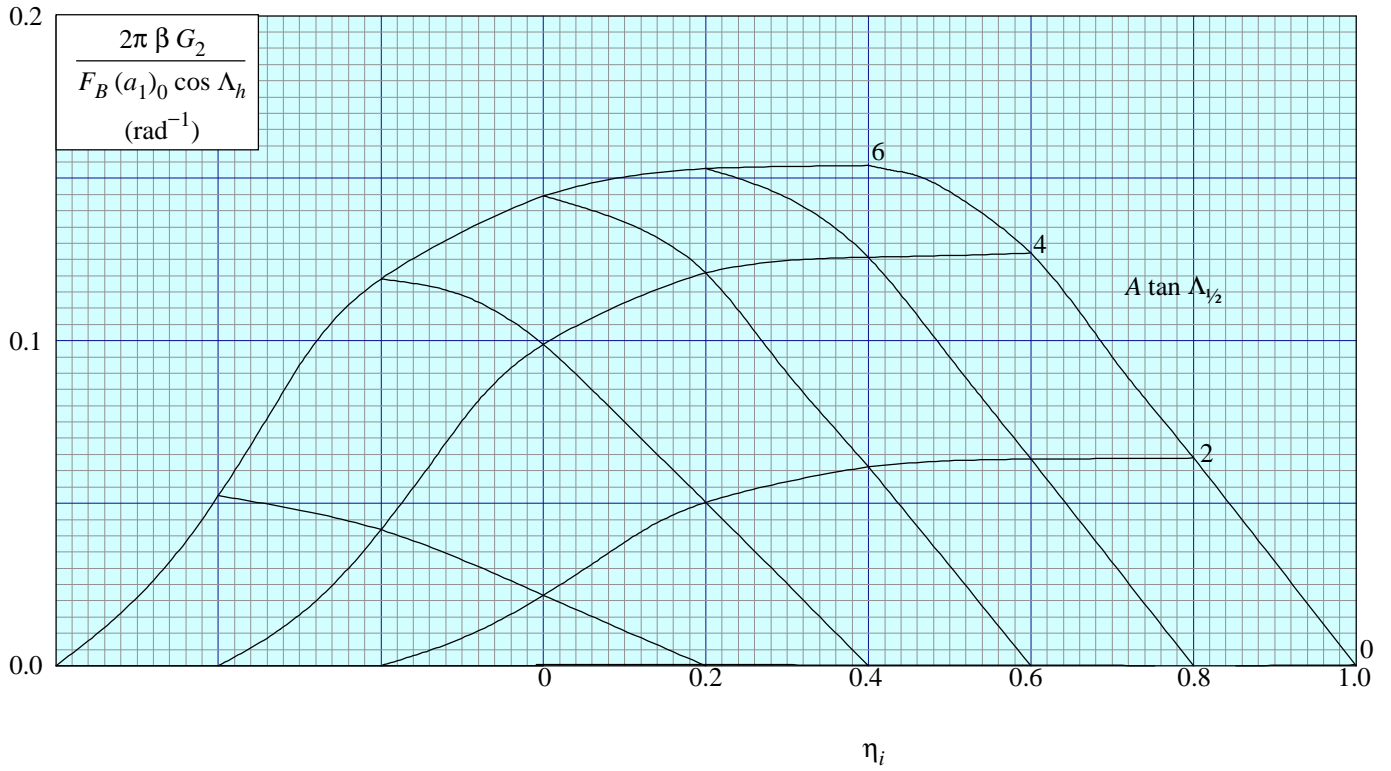
FIGURE 3 INDUCED CAMBER PART-SPAN CORRECTION FOR b_1

$$\frac{2\pi\,\beta\,G_3}{F_B\,(a_1)_0\,\cos\Lambda_h}\ (\mathrm{rad}^{-1})$$
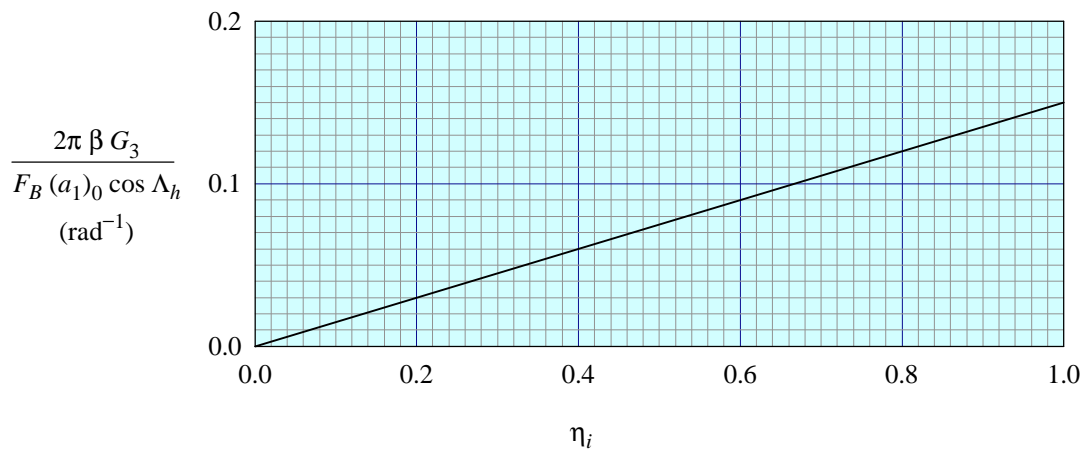
**FIGURE 4 ADDITIONAL PART-SPAN CORRECTION FOR b_2**
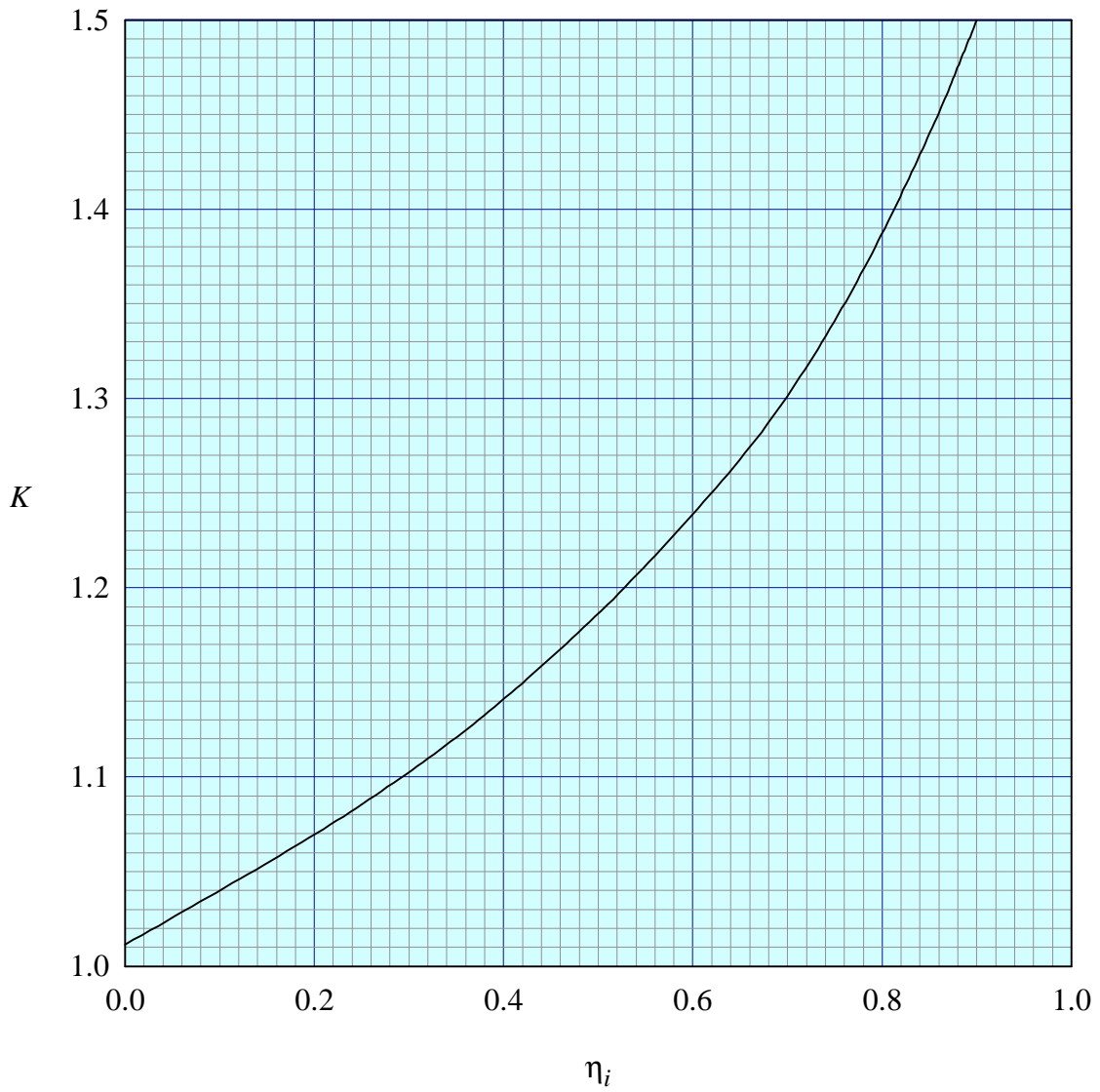
FIGURE 5 INDUCED ANGLE OF ATTACK CORRECTION FACTOR FOR RECTANGULAR WINGS

THE PREPARATION OF THIS DATA ITEM

The work on this particular Item, which supersedes Item No. Aero C.04.01.05 and in part Item No. Aero C.04.01.00, was monitored and guided by the Aerodynamics Committee which first met in 1942 and now has the following membership:

Chairman
Mr H.C. Garner   –   Independent

Vice-Chairman
Mr P.K. Jones   –   British Aerospace (Commercial Aircraft) Ltd, Woodford

Members
Mr G.E. Bean[*]   –   Boeing Aerospace Company, Seattle, Wash., USA
Dr N.T. Birch   –   Rolls-Royce plc, Derby
Mr E.A. Boyd   –   Cranfield Institute of Technology
Mr K. Burgin   –   Southampton University
Dr T.J. Cummings   –   Short Brothers plc
Mr J.R.J. Dovey   –   Independent
Mr L. Elmeland[*]   –   Saab-Scania, Linköping, Sweden
Dr J.W. Flower   –   Independent
Mr P.G.C. Herring   –   Sowerby Research Centre, Bristol
Mr R. Jordan   –   Aircraft Research Association
Mr J.H. Kraus[*]   –   Northrop Corporation, Hawthorne, Calif., USA
Mr J.R.C. Pedersen   –   Independent
Mr R. Sanderson   –   Messerschmitt-Bölkow-Blohm GmbH, Bremen, W. Germany
Mr A.E. Sewell[*]   –   McDonnell Douglas, Long Beach, Calif., USA
Mr M.R. Smith   –   British Aerospace (Commercial Aircraft) Ltd, Bristol
Miss J. Willaume   –   Aérospatiale, Toulouse, France.

[*]   Corresponding Member

The technical work in the assessment of the available information and the construction and subsequent development of the Data Item was carried out by

Mr R.W. Gilbey   –   Senior Engineer.